Smart Structures and Systems, *Vol. 35*, *No. 1* (*2025*) *1-13*
https://doi.org/10.12989/sss.2025.35.1.001

Multi-mode vibration control of substation steel pipe lightning rods by multi-mode TMDs

Junchen Ye [1,2a], Huawei Niu[*1,2], Jinlin Chen [1,2b], Fengli Yang [3c], Guo Huang [3d], Zhengqing Chen [1,2e], Guowen Ran [4], Linwei Ding [4], Hong Tang [4] and Xi Zhang [4]

[1] *State Key Laboratory of Bridge Engineering Safety and Resilience*, *Changsha*, *Hunan*, *410082*, *China*
[2] *Key Laboratory for Bridge and Wind Engineering of Hunan Province*, *Hunan University*, *Changsha 410082*, *China*
[3] *China Electric Power Research Institute*, *Beijing*, *100055*, *China*
[4] *Central China Branch of Guangdong Energy Group Guizhou Co*., *Ltd*, *Changsha*, *Hunan*, *410000*, *China*

(*Received March 19*, *2024*, *Revised October 13*, *2024*, *Accepted December 22*, *2024*)

Abstract. A novel multi-mode eddy current tuned mass damper (TMD) is proposed and designed to effectively control wind-induced vibrations of substation lightning rod structures. The TMD eliminates the need for springs and utilizes the resonant characteristics of a cantilever beam and a single pendulum, enhancing spatial efficiency. Rigorous validation through on-site measurements confirms the vibration reduction performance of the TMD. The modal damping ratios of the top ten modes for steel pipe structure of the substation lightning rod generally remain below 3‰. The multi-mode TMD significantly reduces the root-mean-square (RMS) acceleration response of the original lightning rod structure by 50%, and increases the modal damping ratio of each target mode by 5‰ on average. The additional modal damping of the fourth mode reaches 1%. The state space equation of the TMD-structure model is established, and the TMD design steps considering the additional mass of the device are proposed based on the complex mode analysis. The optimization of the TMD parameters (mass ratio, frequency ratio and damping ratio) is performed to minimize the response of the structure under wind excitation. With the increase of mass ratio, mode order and structure damping ratio, the optimal frequency ratio decreases, but the optimal damping ratio increases. It is necessary to set the corresponding optimal frequency ratio and optimal damping ratio by global optimization to ensure the optimal damping effect of TMD.

Keywords: field measurement; lightning rod; modal damping ratio; TMD; vibration control

1. Introduction

As an indispensable intermediary in power transmission and distribution, substations play a significant role in voltage conversion, power exchange, and electric energy distribution. The reliable operation of these substations is the foundation of the interconnected grid systems. Lightning rods, usually designed as independent steel pipes, are generally applied in substations as a lightning protection measure. However, there is a burgeoning risk of widespread power outages arising from wind-induced collapses of these steel pipe lightning rods. Such collapses can compromise the integrity of adjacent substation infrastructure and impede the consistent operation of the broader power system, potentially culminating in grid shutdowns with consequential impacts on construction, living standards, emergency responses, and even instigating secondary catastrophic events. Circa 2015, China witnessed a spate of wind-induced fracturing and collapsing incidents involving steel pipes in cross-regional substations in Xinjiang and Gansu Provinces. These events covered a voltage spectrum from 220 kV to 750 kV and caused severe damage to power transport in local areas. Therefore, there is an urgent need to examine the wind resilience of these lightning rods to ensure the effective operation of substations.

The independent steel pipe lightning rod has features of pronounced aspect ratio, inherent pliability, and minimal damping capabilities (Pagnini and Solari 2001), which is susceptible to wind buffeting and aerodynamic perturbations (Mengistu *et al*. 2023). Unlike traditional square or triangular steel lightning rods, the steel pipe lightning rod with a circular cross-section is predisposed to consistent vortex shedding at daily wind velocities, and may result in crosswind resonances due to frequency convergence between the structure and vortices (Tapia-Hernández 2016). In addition, long-term exposure to low-intensity cyclic wind forces can also weaken the mechanical resilience of steel pipe lightning rods. The fatigue issue may induce fissures or complete ruptures at stress points (Zhao *et al*. 2022). Thus, as presented by previous studies (Repetto and Solari 2010), this anti collapse challenge involves many fields, e.g., meteorological, aerodynamic, and mechanical domains. To address it, Nguyen *et al*. (2015) conducted

*Corresponding author, Ph.D., Professor,
E-mail: niuhw@hnu.edu.cn
[a] Ph.D. Student
[b] Ph.D. Student
[c] Ph.D.
[d] Ph.D.
[e] Ph.D.

ISSN: 1738-1584 (Print), 1738-1991 (Online)

experimental studies on the aerodynamic stability of slender vertical structures and their responses to wind stimuli and highlighted the importance of vibration mitigation. Furthermore, to investigate wind vibration control of slender cylindrical structures, many different methods have been developed in recent decades, including aerodynamic measures, mechanical measures, and damper measures.

The aerodynamic measures such as wake splitter plates (Xu *et al*. 2024), spiral protuberances (Dao *et al*. 2023), helical strakes (Quen *et al*. 2018), active local blowing (Maryami *et al*. 2024) and bionic surface (Chen *et al*. 2022) are proposed to reduce the response by changing the flow pattern around the structure. The aerodynamic measures have low cost and strong operability, but in the design process, it is necessary to compare different aerodynamic shapes through wind tunnel tests to determine the optimal scheme and avoid adverse effects on other types of wind induced vibration of the structure. In practical engineering, the aerodynamic measures are often combined with other measures.

The mechanical measure is usually referred to as using auxiliary cables or supports to change the structural natural frequency. However, this measure will increase the construction cost and the footprint. Thus, it is not recommended to use mechanical measures to control wind vibration in existing lightning rod of substations.

The damper measure is to install a damper on the objective structure to absorb and consume vibration energy, which is the most widely used method in wind-induced vibration control of vertical structures. Several types of damping measures have been developed, including impact dampers (Cook *et al*. 2001, Caracoglia and Jones 2007), viscous dampers (Hamilton *et al*. 2000, McManus *et al*. 2003), tuned liquid damper (Zhou *et al*. 2023) and tuned mass damper (McManus *et al*. 2003, Christenson *et al*. 2014, Kontoni and Farghaly 2020). Tuned mass damper, referred to as TMD, typically only addresses a specific modal vibration. However, the lightning rods exhibit multimodal vibration under wind loads because of their light weight and high flexibility (Han *et al*. 2021). Therefore, a single TMD is unable to fully suppress the multi-order wind-induced vibration of the lightning rod.

In this work, a novel multi-modal eddy current TMD is proposed to address the issue of the multi-order wind-induced vibration of steel pipe lightning rods. The state space equation of the TMD-structure model is first established to analyze the dynamic characteristics of the system. According to the complex mode analysis, the TMD design is then developed considering the additional mass of the device. In addition, the Red-tailed hawk algorithm (RTH) global optimization method is used to find the optimal parameters for the multi-mode TMD. Finally, the dynamic characteristics of a field structure are measured before and after the installation of TMD. The result verifies the effectiveness of the proposed multi-mode TMD, which provides a valuable reference for damping schemes of similar structures.

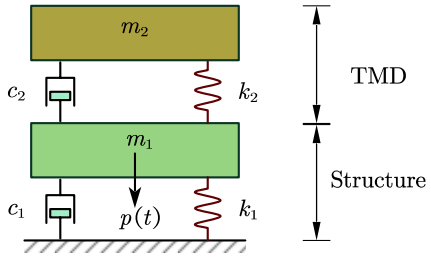

Fig. 1 The schematic diagram of the main structure-TMD coupled system model

2. Design and calculation of multi-mode TMD for steel pipe lightning rods

2.1 Single TMD design theory

TMD is a device consisting of mass, spring, and damping elements that assists structures in reducing structural vibrations by absorbing external energy. When the natural frequency of the TMD closely matches that of the objective structure, TMD will generate inertial forces, effectively reducing the vibration response of the structure. The schematic diagram of the Single Degree of Freedom (SDOF) structure-TMD coupled system model is shown in Fig. 1, and the governing equation describing such a system can be expressed as

$$m_1\ddot{x}_1 + c_1\dot{x}_1 + k_1x_1 - c_2(\dot{x}_2 - \dot{x}_1) - k_2(x_2 - x_1) = p(t) \quad (1)$$

$$m_2\ddot{x}_2 + c_2(\dot{x}_2 - \dot{x}_1) + k_2(x_2 - x_1) = 0 \quad (2)$$

where m_1, c_1 and k_1 represent the structural mass, damping, and stiffness, respectively; m_2, c_2 and k_2 denote the mass, damping, and stiffness of the TMD system, respectively; $\ddot{x}_1$, $\dot{x}_1$ and x_1 refer to the structural acceleration, velocity, and displacement, respectively; $\ddot{x}_2$, $\dot{x}_2$ and x_2 refer to acceleration, velocity, and displacement of the TMD system, respectively; p(t) represents the external load acting on the structure.

The dynamic amplification coefficient (the ratio of the dynamic response amplitude to the static response amplitude) can be obtained using the transfer function method. Considering the dynamic amplification coefficient as the optimization index, the optimal frequency ratio α_{opt} (the ratio of the TMD's natural frequency to the structure's natural frequency) and the optimal damping ratio ξ_{opt} (the energy dissipation capacity of the TMD) can be obtained by minimizing this coefficient. The optimal parameters of TMD under different excitation and optimization objectives are listed in Table 1 (Constantinou *et al*. 1998).

2.2 Multi-mode TMD for steel pipe lightning rods

As mentioned before, the lightning rods exhibit multi-mode vibrations at daily wind velocity due to their flexibility. A multi-mode TMD is required to suppress the multi-order wind-induced vibration. However, due to the

Table 1 Optimum parameters of TMD under different excitation and optimization objectives

Case	Excitation		Optimized Response		Optimized Absorber Parameter	
	Type	Applied to	Optimization objective	R_{opt}	α_{opt}	ξ_{opt}
1	$f_0 \sin \omega t$	Structure	$\frac{kx}{f_0}$	$\left(1+\frac{2}{\mu}\right)^{\frac{1}{2}}$	$\frac{1}{1+\mu}$	$\sqrt{\frac{3\mu}{8(1+\mu)}}$
2	$f_0 \sin \omega t$	Structure	$\frac{m\ddot{x}}{f_0}$	$\left(\frac{2}{\mu(1+\mu)}\right)^{\frac{1}{2}}$	$\left(\frac{1}{1+\mu}\right)^{\frac{1}{2}}$	$\sqrt{\frac{3\mu}{8(1+\mu/2)}}$
3	$\ddot{x}_g \sin \omega t$	Base	$\frac{\omega^2 x}{x_g}$	$\left(\frac{2}{\mu}\right)^{\frac{1}{2}}(1+\mu)$	$\frac{(1-\mu/2)^{1/2}}{1+\mu}$	$\sqrt{\frac{3\mu}{8(1+\mu)(1-\mu/2)}}$
4	$\ddot{x}_g \sin \omega t$	Base	$\frac{\ddot{x}_g+\ddot{x}}{\ddot{x}_g}$	$\left(1+\frac{2}{\mu}\right)^{\frac{1}{2}}$	$\frac{1}{1+\mu}$	$\sqrt{\frac{3\mu}{8(1+\mu)}}$
5	Random white noise force	Structure	$\frac{<x^2>k^2}{2\pi S_0 \omega_s}$	$\sqrt{\frac{1+3\mu/4}{\mu(1+\mu)}}$	$\frac{(1+\mu/2)^{1/2}}{(1+\mu)}$	$\sqrt{\frac{\mu(1+3\mu/4)}{4(1+\mu)(1+\mu/2)}}$
6	Random white noise acceleration	Base	$\frac{<x^2>\omega_s^3}{2\pi S_0}$	$(1+\mu)^{3/2}\left(\frac{1}{\mu}-\frac{1}{4}\right)^{1/2}$	$\frac{(1-\mu/2)^{1/2}}{(1+\mu)}$	$\sqrt{\frac{\mu(1-\mu/4)}{4(1+\mu)(1-\mu/2)}}$

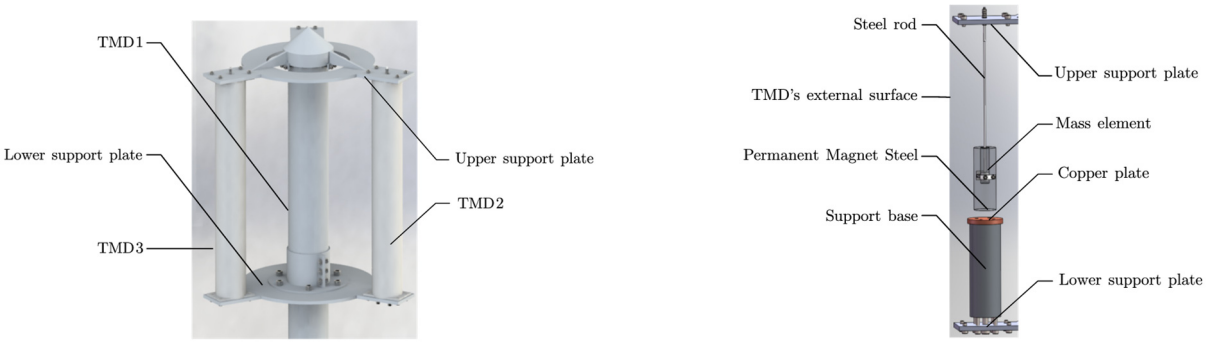

(a) External structure (b) Internal structure of each sub-TMD

Fig. 2 Installation schematic of TMD

limited space of the lightning rod, it is impossible to install the vibration damping device inside the structure like the traditional vibration control scheme of building structures. In this work, a novel external multi-mode TMD device system is designed and manufactured as shown in Fig. 2. The device is composed of three sub-TMDs to control the first three vibration modes of the lightning rod respectively. It achieves a greater range of motion than the spring in the same space.

As shown in Fig. 2, the multi-mode TMD consists of three sets of single TMD components which comprise four key components, i.e., support unit (the support plates and the support base), mass unit (the mass element), damping unit (the relative motion between the copper plate and the magnets generating eddy currents and providing damping), and spring unit (either a cantilever beam or a single pendulum). The pendulum acts as a pinned-free oscillator, allowing rotation at one end and free movement at the mass-attached end. The cantilever beam is a fixed-free oscillator, clamped at one end to prevent all motion, while the mass-attached end is free. These different constraints result in distinct natural frequencies for each spring type, dependent on their physical properties and the attached mass. Three components are uniformly arranged along the circumferential direction of the lightning rod. The angular spacings between the components are 120 degrees. The TMD is connected to the lightning rod through devices such as clamps and support plates. The solid steel rod is rigidly attached to the support plate at the top, while the lower part is connected to the mass block and copper plate.

The eddy current damping is used as the damping element. When the main structure vibrates, the copper plate in the TMD cuts the magnetic inductance lines and produces eddy currents and magnetic resistance force (Liu *et al*. 2020). The movement of the mass block converts external kinetic energy into thermal energy consumption, effectively mitigating the lightning rod's vibration and preventing structural damage. The device operates in a magnetic field and does not require an external power source. In addition, there is no contact between moving

components, thereby reducing potential maintenance.

2.3 Relative displacement calculation of multi-mode TMD

For safety considerations, it is crucial to control the displacement of the TMD within an acceptable range in practice. Alternatively, additional cushioning rubber around the TMD device can prevent the impact force from excessive movement. When the structure vibrates close to the resonance state, there is a 90° phase difference between the external load and the dynamic displacement of the main structure. Therefore, the work done by the external load in one vibration period is

$$W = \pi P_0 x_{max} \tag{3}$$

where P_0 and $x_{\max}$ represent the force and the structural maximum displacement, respectively. The energy dissipation of TMD in one period is

$$W_{\text{dissipated}} = \pi c_{\text{opt}} \omega_{\text{TMD}} x_{\text{rel}}^2 \tag{4}$$

where ω_{TMD} and x_{rel} is the frequency and the relative displacement of TMD, respectively. c_{opt} is the damping coefficient of the TMD. When W and $W_{\text{dissipated}}$ are equal, one can obtain

$$x_{\text{rel}}^2 = \frac{P_0 x_{max}}{c_{\text{opt}} \omega_{\text{TMD}}} \tag{5}$$

Combined with $P_0 = kx_{\text{st}}$, $k = m\omega_s^2$, $\xi_{\text{opt}} = c_{\text{opt}}/c_c$ where x_{st}, k, w_s, m are the structural static displacement, structural stiffness, modal frequency and mass, respectively. ξ_{opt} and c_c are the optimal damping ratio and the critical damping ratio of TMD, respectively.

The above equation can be re-written as follows

$$\left(\frac{x_{\text{rel}}}{x_{max}}\right)^2 = \sqrt{\frac{\mu}{\mu+2}} \times \frac{1}{2\mu} \times \frac{1}{\xi_{\text{opt}}} \times \frac{1}{\alpha_{\text{opt}}^2} \tag{6}$$

where x_{rel} is the relative displacement of TMD. $x_{\max}$ represents the structural maximum displacement. μ is the mass ratio. ξ_{opt} and α_{opt} are the optimal damping ratio and the optimal frequency ratio, respectively.

According to the above equation, the relative displacement between the TMD mass and the main structure can be directly calculated from the mass ratio. That is to say, the motion space of TMD is determined by relative displacement.

3. Field measurement of structure-TMD system

3.1 Field test scheme

In this study, the field measurement is carried out to investigate the validity of the proposed multi-mode TMD for steel pipe lightning rods. The structural wind-induced accelerations are measured at different locations. The field steel pipe lightning rod of a substation is located at northwest China. The field photo and illustration of the on-site structural configuration are shown in Fig. 3.

Considering the limitation of the field conditions, both free vibration method and environment excitation method are used to test the dynamic characteristics of the lightning rod. The Lens LC0166C piezoelectric accelerometer is used in this test, with a frequency range of 0.1 Hz–2000 Hz, a sensitivity of about 1000 mV/g, and a single mass of 182 mg. The data acquisition system is DH8302. The Kestrel 5500 LINK wind speed meteorologist is used for wind speed measurement, with a range of 0.6-40 m/s. The automatic storage interval of this meteorologist is 2 seconds to 12 hours, and the test data is transmitted wirelessly via

(a) Field photo

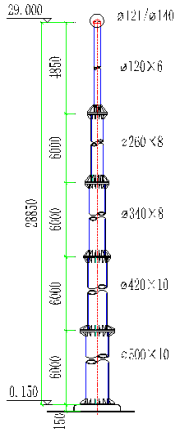

(b) Outline drawing

Fig. 3 Field photo and illustration of independent lightning rod

(a) LC0166C

(b) DH8302

(c) Kestrel 5500 LINK

Fig. 4 Field test photos

Bluetooth. Two acceleration sensors are installed at the top of the structure in an orthogonal direction, named the x and y axes. The sampling frequency is 200 Hz. The crane is used to transport workers and sensor equipment to the top of the structure, where the sensors are installed to the structure via a magnetic base. The equipment photos are shown in Fig. 4.

3.2 Dynamic characteristics without TMD

The dynamic characteristics of the independent lightning rod are first obtained through both free vibration analysis and environmental excitation, including the natural frequency and damping ratio. The typical time history and spectrum results of the dynamic characteristics test of steel pipe lightning rods are plotted in Fig. 5.

During the testing, there were no strong winds. The wind speed at the top of the steel pipe structure was measured from 2 m/s to 3 m/s. In addition, the low sampling frequency of wind speed makes it difficult to calculate its spectral characteristics. More investigation is recommended to further explore the wind environment of the steel pipe lightning rod in the substation.

Modal damping ratio is a crucial but uncertain parameter in structural dynamics, which significantly influences the dynamic response, particularly for tall, slender structures like lightning rods. To determine this parameter, both free-decay acceleration signals and environmental vibration signals were analyzed. For the free-decay analysis, the measured signals were directly obtained after an initial excitation was applied to the structure. The measured signals are subjected to bandpass filtering and the cutoff frequency is set near the target frequency to generate a single-frequency decaying vibration signal. In this way, a series of free decay curves are obtained corresponding to different vibration amplitudes, which are considered as the free vibration signals. The power spectral analysis is then applied to the filtered signal to yield the dominant frequency, and the logarithmic decrement method can be used to calculate the corresponding modal damping ratio.

In practice, the Random Decrement Technique (RDT) is generally used to address the intricate frequency components of the environmental excitation signal (Thiyagarajan *et al*. 2021, Wen *et al*. 2018). This method involves extracting the sub-signals from the original vibration signals using the Analytical Mode Decomposition (AMD) technique. By utilizing the random decrement signature derived from these sub-signals, the RDT method can accurately identify the structural dynamic parameters, including the modal damping ratio. Overall, this refined approach can provide a more accurate determination of the damping characteristics under complex environmental excitation. In this way, both free vibration signals and environmental vibration signals are analyzed up to the tenth mode, and the results are listed in Table 2. The observed frequency equivalence in mode pairs, such as 1 and 2, is a consequence of the lightning rod's symmetrical design. These modes correspond to orthogonal vibration directions (e.g., X and Y), with frequencies that are effectively identical within the limits of measurement precision.

Both excitation methods effectively capture the first 10 modal frequencies of the lightning rod. In fact, the independent lightning rod exhibits abundant identified frequencies. Here only the first 10 modes are presented. The modal damping ratios of the top ten modes are determined

Table 2 Summary of the first 10 modal parameters of lightning rod without TMD

Order	Free vibration method		Environmental vibration method	
	Frequency /Hz	Damping ratio	Frequency /Hz	Damping ratio
1	0.781	0.266%	0.786	0.141%
2	0.781	0.052%	0.792	0.106%
3	2.930	0.178%	2.883	0.068%
4	2.930	0.153%	2.902	0.030%
5	5.469	0.345%	5.541	0.013%
6	5.469	0.270%	5.583	0.017%
7	9.570	0.202%	9.568	0.011%
8	9.570	0.043%	9.640	0.022%
9	16.990	0.336%	16.872	0.004%
10	16.990	0.112%	16.988	0.017%

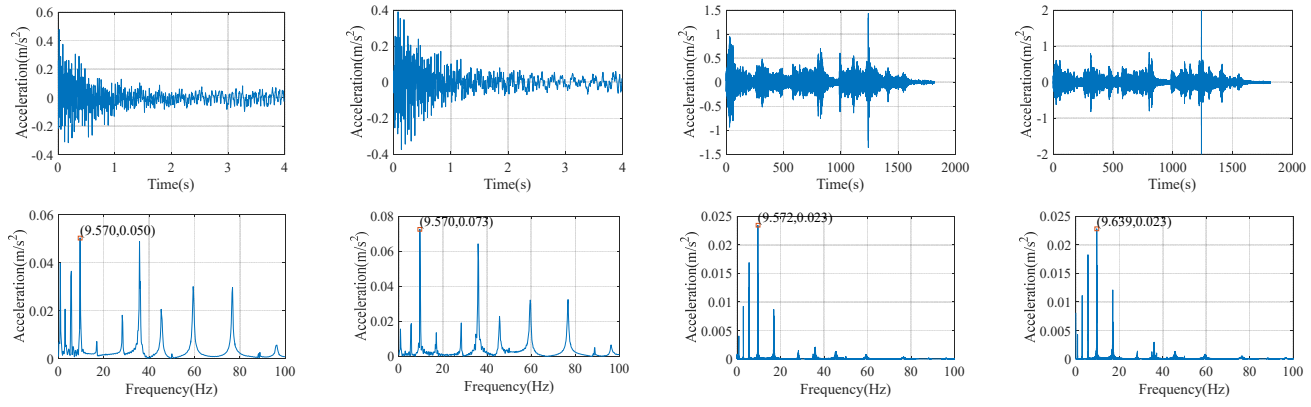

(a) X-Free vibration (b) Y-Free vibration (c) X-Environmental vibration (d) Y-Environmental vibration

Fig. 5 Time history and FFT of free vibration and environmental vibration without TMD

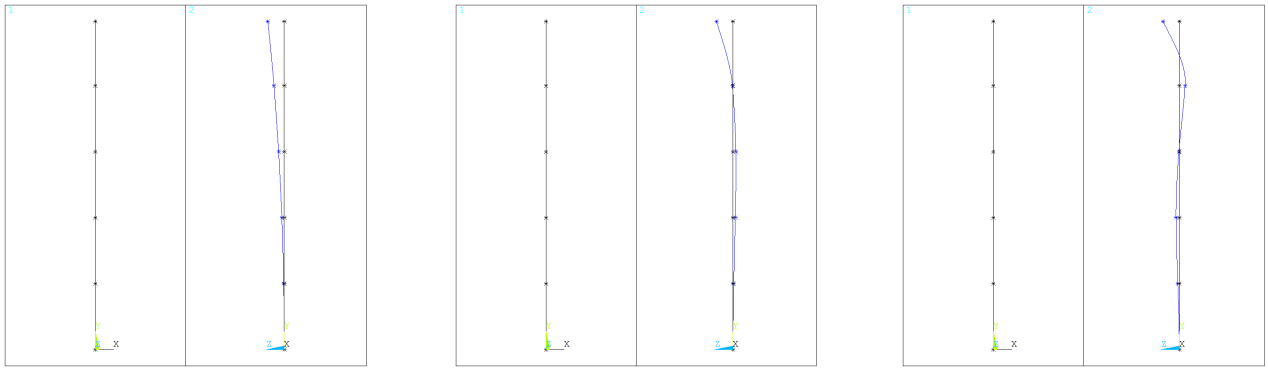

(a) 1st order (b) 2nd order (c) 3rd order

Fig. 6 The first three modes of steel pipe lightning rod

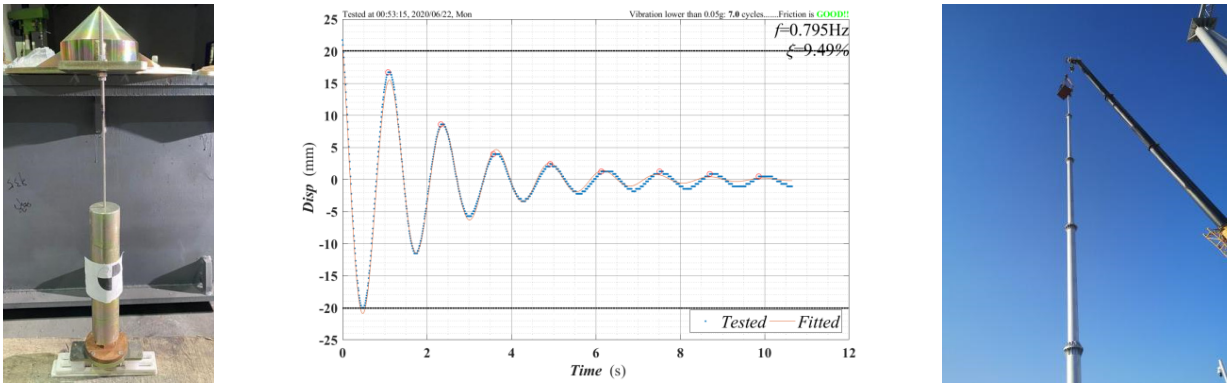

(a) Calibration photo (b) Calibration result (c) Installation of TMD

Fig. 7 Calibration and installation of TMD

through numerous repeated tests and the values are generally below 3‰, consistent with the results of previous studies (Solari and Pagnini 1999). The low damping characteristics may lead to the occurrence of micro wind-induced vibrations in the structure. Given the susceptibility of closely spaced natural frequencies to induce multi-mode vibrations, mitigation measures are necessary. Consequently, a Tuned Mass Damper (TMD) will be employed on the lightning rod to suppress these undesirable vibrations.

3.3 Installation location of TMD

To achieve the maximum vibration reduction effect, TMD should be installed at the location where the modal vibration displacement of the structure is maximum. To this end, the finite element model of the lightning rod is established using ANSYS software. The steel pipe is modeled with the Beam188 unit. This unit is suitable for simulating the thin beam structure based on a 3D finite strain beam. In addition, the additional masses such as flanges and bolts are modeled as the Mass21 unit which acts on the structure as the concentrated mass. To ensure the consistency of the total mass of the structure, the remaining mass is distributed throughout the entire structure in the form of equivalent density. Each connection is considered as a rigid connection. The eigenvalue solver of the Block Lanczos method is used to obtain the mode shape of this model, as shown in Fig. 6. It is found that for the first three mode shapes, the maximum displacement occurs at the top of the structure. Therefore, the proposed TMD is recommended to install on the top of the structure to achieve optimal vibration reduction effectiveness. It should be noted that the first three modal masses of the lightning rod are 268.86 kg, 87.48 kg and 54.63 kg, respectively. The total mass of the lightning rod is 2096.79 kg, consistent with the statistical mass of design drawings.

3.4 Design, calibration and installation of TMD

The first order TMD is designed as a single pendulum structure, hinged at the connection point, to reduce the total length to achieve low design frequency. The second and the third order TMDs are designed as segmented cantilevers, as shown in Fig. 7(a), adjusting the length and diameter of each segment to achieve the target frequency. All TMDS are made of stainless steel. Each TMD oscillates in multiple directions to control vibrations from various wind directions. According to the first three structural frequencies obtained in the field measurement and the first three structural modal masses in the FEM, the optimal parameters of TMD are obtained by the formula in case 1 of Table 1. The parameters design results of TMD are listed in Table 3.

Before installation, the dynamic characteristics of each

Table 3 Parameters of TMD design for field measurement

No.	Support type	Segment 1		Segment 2		Segment 3		Total length /m	Mass /kg	*f*/Hz	ξ
		Radius /m	Length /m	Radius /m	Length /m	Radius /m	Length /m				
1	Single pendulum	0.005	——	——	——	——	——	0.430	6	0.766	9.05%
2	Segmented cantilever	0.005	0.063	0.003	0.237	0.025	0.195	0.495	3	2.809	11.15%
3	Segmented cantilever	0.005	0.129	0.004	0.171	0.025	0.195	0.495	3	5.219	13.97%

*The order of segment in the table from left to right is the TMD fixed end to free end direction

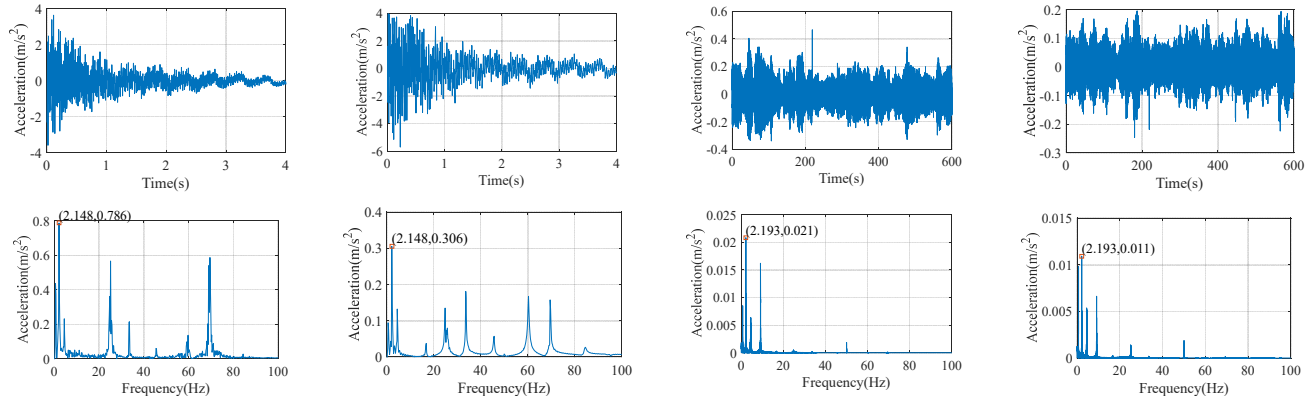

(a) X-Free vibration (b) Y-Free vibration (c) X-Environmental vibration (d) Y-Environmental vibration

Fig. 8 Time history and FFT of free vibration and environmental vibration with TMD

TMD were calibrated. The speckle identification of the moving end was carried out by a high-speed camera, and the structural frequency and damping ratio were obtained by the free attenuation curve. The TMD is installed on the top of the structure in the field and secured by a hoop on the bottom plate. Typical calibration and installation photos are shown in Fig. 7.

3.5 Dynamic characteristics with TMD

After the installation of TMD, the dynamic characteristics of the independent lightning rod were also obtained through free vibration analysis and environmental excitation, including natural frequency and damping ratio. The test was repeated three times to remove the influence of random factors as much as possible. Typical time history and corresponding spectrum results are shown in Fig. 8.

Similarly, the rearranged results of the modal frequencies and damping ratios for the top ten modes of the steel pipe lightning rod under both the free vibration method and environmental random excitation are listed in Table 4. The modal frequencies obtained from the free vibration method are consistent to those of the environmental excitation method. The identification error is generally within 5%. After the TMD installation, the low-order modal frequencies decrease, which can be attributed to an increase in the equivalent modal mass of the structure. Additionally, the modal damping ratio is significantly increased for all target modes, with an average increase of 5‰. The additional modal damping of the fourth mode reaches 1%. This improvement will help ensure the safety and stability of the lightning rod under wind loads. Moreover, since the damping ratio of the first ten modes of the structure is all improved, it also indicates that the multi-order TMD has a better frequency action range than a single TMD.

Table 4 Summary of the first 10 modal parameters of the lightning rod with TMD

Order	Free-decay method		Environmental vibration method	
	Frequency /Hz	Damping ratio	Frequency /Hz	Damping ratio
1	0.684	0.548%	0.665	0.873%
2	0.684	0.320%	0.675	0.896%
3	2.148	0.583%	2.188	-
4	2.148	1.272%	2.188	-
5	4.590	1.171%	4.489	0.044%
6	4.492	0.708%	4.519	0.150%
7	9.180	0.423%	9.126	0.027%
8	16.700	0.418%	9.166	0.008%
9	24.800	0.482%	25.121	0.005%
10	25.089	0.238%	-	-

(a) X direction (b) Y direction

Fig. 9 Comparison of wind vibration response before and after TMD installation

4. Analysis of multi-mode TMDs' vibration reduction effect

4.1 Vibration reduction effect in field measurement

In order to more intuitively and quantitatively assess the vibration reduction effect of the TMD device on the lightning rod, a case associated with the comparison of the wind-induced accelerations between two independent steel lightning rods was considered. Those two lightning rods are located at the tested substation with the same configuration. Their height is 29 m, and one of them has the proposed TMD devices and the other does not. The time-domain comparisons of the along-wind and cross-wind directions are shown in Fig. 9.

As shown, it is evident that the TMD device has a significant vibration reduction effect on the wind-induced response. After the TMD installation, the root-mean-square value of the accelerations is decreased by 46.92% and 52.34% in orthogonal directions, respectively. The result concludes that the TMD device can effectively reduce the dynamic response of the structure under wind loads, thereby reducing the probability of failure and collapse accidents. These are crucial to ensure the reliability and safety of the substation lightning rod structure under wind-induced vibrations.

4.2 The influence of the TMD device mass

Comparing the frequency results in Table 2 and Table 4, it can be seen that the 1st order frequency of the structure was reduced by more than 10% after the installation of TMD, and the frequencies of other modes decrease more dramatically. This indicates that there is a mismatch between the frequency of TMD and the main structure, which will cause TMD to be unable to fully exert its damping effect. The key finding is the added mass of the TMD device, such as the shell, bottom plate, etc. This component is designed to ensure that the TMD can work normally. In fact, it does not participate in the TMD movement. However, it acts on the top of the structure in the form of concentrated mass, which will have a great impact on the dynamic characteristics of the structure. In order to verify this hypothesis, the structure-TMD finite element model is established in this section for further analysis.

The total weight of the TMD device is 57 kg, of which 45 kg is the additional mass, including the bottom plate, the shell and the connector, etc. As mentioned, those masses do not participate in the TMD vibration reduction work. In finite element analysis, an additional device is applied to the top of the structure in the form of concentrated mass to analyze the dynamic characteristics. The results of the first six modal frequencies measured in the field compared with those of the finite element model are listed in Table 5.

Table 5 Comparison of the first six modal frequencies

Order	Original structure			Considering additional mass of TMD		
	Field	FEM	Error	Field	FEM	Error
1	0.783	0.758	3.19%	0.684	0.698	2.16%
2	0.786	0.758	3.56%	0.684	0.698	2.16%
3	2.906	2.687	7.54%	2.148	2.175	1.27%
4	2.911	2.687	7.69%	2.148	2.175	1.27%
5	5.506	4.991	9.35%	4.590	4.189	8.74%
6	5.506	4.991	9.35%	4.492	4.189	6.74%

When the additional masses are not considered, the frequencies of the finite element model show a certain degree of error (within 10%) compared to that of the field test. When the additional masses are considered, the predicted frequencies of the finite element model are improved to some extent. Admittedly, there are still errors between the finite element model and the field test. Those errors may be caused by some differences in the constraints, connections or component forms of the two. Nevertheless, the result verifies that the structure frequency is greatly reduced after TMD installation, which is mainly affected by the mass of the TMD device.

4.3 Design process of Multi-mode TMDs for steel pipe lightning rods

It should be noted that there are significant differences in TMD design of large structures such as bridges or buildings, and flexible vertical structures such as steel pipe lightning rods. Because the additional mass of TMD are negligible relative to the former, but not for the latter. The mass of the TMD device is several times the TMD motion mass leading to the structural frequency reduction of more than 10%. In other words, if the TMD is still designed according to the dynamic characteristics of the original structure, the TMD frequency will be out of tune with the

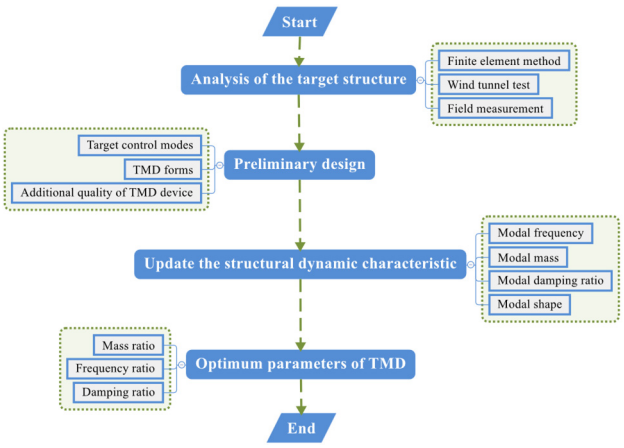

Fig. 10 Flow chart of TMD design

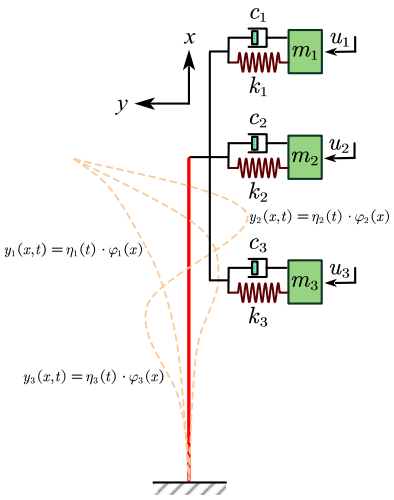

Fig. 11 Diagram of the structure-TMDs system

original structure frequency, and the vibration damping performance of the TMD will be significantly reduced. Therefore, for light and flexible vertical structures such as lightning rods, the mass of additional devices has to be considered in the process of the TMD design. In this way, the design process of TMD is re-adjusted as shown in Fig. 10.

5. Structure-TMD finite element model and complex modal analysis

5.1 FEM of Structure-TMDs

A cantilever beam with three TMDS is considered. Fig. 11 depicts the layout of the system. The mass units of each TMD are connected to the top of the structure by linear springs and dampers, which control the first three modes of vibration respectively. The displacement of the structure can be described by the superposition method as a combination of multiple modes, as shown by the dotted line.

The equation of free vibration motion for the Structure-TMDs is derived using the principle of virtual work

$$\int_L \left[m_s(x)\frac{\partial^2 y_s(x,t)}{\partial t^2} + c_s(x)\frac{\partial y_s(x,t)}{\partial t} + \mathrm{EI}(x)\frac{\partial^4 y_s(x,t)}{\partial x^4}\right]\cdot\delta y_s(x,t)dx + \sum_{j=1}^{3}\left[c_j\left[\frac{\partial y_s(x,t)}{\partial t} - \frac{\partial u_j(t)}{\partial t}\right] + k_j\left[y_s(x,t) - u_j(t)\right]\right]\cdot\delta y_s(x,t) = 0, \qquad j = 1,2,3 \tag{7}$$

$$\left[m_j\frac{\partial^2 u_j(t)}{\partial t^2} - c_j\left[\frac{\partial y_s(x,t)}{\partial t} - \frac{\partial u_j(t)}{\partial t}\right] - k_j\left[y_s(x,t) - u_j(t)\right]\right]\cdot\delta u_j(t) = 0, \qquad j = 1,2,3 \tag{8}$$

where $m_s(x)$, $c_s(x)$, and EI(x) represent the distributed mass, distributed damping coefficient, and bending stiffness of the structure, m_j is the mass element of TMD, $y_s(x,t)$ is the displacement of the structure at the height of x, $u_j(t)$ is the displacement of TMD, and $\delta y_s(x,t)$ and $\delta u_s(x,t)$ are the virtual displacement of structure and TMD.

The structure displacement is decomposed into the sum of modal displacement by the superposition principle

$$y_s(x,t) = \sum_n \phi_i(x)\eta_i(t) \tag{9}$$

where $\varphi_i(x)$ and $\eta_i(t)$ represent the modal shape and the time history of modal displacement of the ith mode, respectively.

After installing the TMDs, the main structure will obtain additional modal damping, which can be computed through complex modal analysis. The principle of complex modal analysis is to express the system's free vibration equation in the form of state equations as follows

$$R\dot{z} + Qz = 0 \tag{10}$$

where $z = [\eta\ \dot{\eta}]^T$ represents a state vector, and

$$R = \begin{bmatrix} C^* & M^* \\ M^* & 0 \end{bmatrix}, \qquad Q = \begin{bmatrix} K^* & 0 \\ 0 & -M^* \end{bmatrix} \tag{11}$$

in which M*, C * and K* are the mass, damping, and stiffness matrices of the system, which can be expressed as

$$M * = diag(m_{s1}, \ldots, m_{sn}, m_1, m_2, m_3) \tag{12}$$

where m_{s1}, ..., m_{sn} are the structural modal frequency obtained by modal analysis.

$$\boldsymbol{C}*=\begin{bmatrix} c_{s1}+\sum_{j=1}^{3}c_j & \cdots & \sum_{j=1}^{3}c_j & -c_1 & \cdots & -c_3 \\ \vdots & \ddots & \vdots & \vdots & \ddots & \vdots \\ \sum_{j=1}^{3}c_j & \cdots & c_{sn}+\sum_{j=1}^{3}c_j & -c_1 & \cdots & -c_3 \\ -c_1 & \ldots & -c_1 & c_1 & \ldots & 0 \\ \vdots & \ddots & \vdots & \vdots & \ddots & \vdots \\ -c_3 & \ldots & -c_3 & 0 & \ldots & c_3 \end{bmatrix} \tag{13}$$

$$K*=\begin{bmatrix} k_{s1}+\sum_{j=1}^{3}k_j & \cdots & \sum_{j=1}^{3}k_j & -k_1 & \cdots & -k_3 \\ \vdots & \ddots & \vdots & \vdots & \ddots & \vdots \\ \sum_{j=1}^{3}k_j & \cdots & k_{sn}+\sum_{j=1}^{3}k_j & -k_1 & \cdots & -k_3 \\ -k_1 & \ldots & -k_1 & k_1 & \ldots & 0 \\ \vdots & \ddots & \vdots & \vdots & \ddots & \vdots \\ -k_3 & \ldots & -k_3 & 0 & \ldots & k_3 \end{bmatrix} \tag{14}$$

Let $z = \varphi e^{\lambda t}$

$$(\lambda R + Q)\varphi = 0 \tag{15}$$

The characteristic equation is

$$det(\lambda R + Q) = 0 \tag{16}$$

Solving the above equation, the complex feature roots λ_i and λ_i*, and the corresponding feature vectors ϕ_i and ϕ_i* (i = 1, 2, ..., n) are obtained.

$$\begin{aligned} \lambda_i &= \sigma_i + j\omega_{mi}\sqrt{1-\xi_{mi}^2} \\ &= -\xi_{mi}\omega_{mi} + j\omega_{mi}\sqrt{1-\xi_{mi}^2} \end{aligned} \tag{17}$$

Therefore, the modal frequency ω_{mi} and modal damping ratio ξ_{m_i} can be obtained as follows

$$\omega_{mi} = |\lambda_i| \tag{18}$$

$$\xi_{m_i} = -\sigma_i/\omega_{m_i} \tag{19}$$

5.2 Global optimization for TMDs

The actual wind vibration response of the lightning rod includes buffeting, which can be represented by random loads, and vortex-induced vibration, which can be represented by sinusoidal loads. However, the actual load of the structure is complex, and the damping ratio of the structure cannot be ignored. When multiple TMDs are installed to control the multi-order vibration of the structure, the optimal parameters of the TMDs will affect each other. The traditional optimization formula in Table 1 can no longer meet the actual needs, and an improved method needs to be found to obtain the optimal parameters of the multi-order TMDs. In this study, a global optimization method of multi-order TMD based on additional modal damping ratio is proposed.

The performance of TMD is closely related to the mass ratio μ, frequency ratio α, and damping ratio ξ. The design of the multi-mode TMD aims to find the optimal parameters (frequency ratios and damping ratios) for each sub-TMD that maximize the damping introduced to the critical modes of the lightning rod structure. For given original structural damping ratio ξ_p, the TMDs' mass ratios μ_i, the optimal frequency ratio α_{opt} and the optimal damping ratio ξ_{opt} can be obtained by the global optimization method. The objective function is defined as the maximum of the sum of the weighted minimum modal damping ratios of each order, as shown in Eq. (19). This equation is based on the contribution of TMDs to the modal damping ratio of the structure obtained by the complex modal analysis method.

$$J = \max_{\alpha_1,\alpha_2,\alpha_3,\xi_1,\xi_2,\xi_3} \sum_{i=1}^{3} \rho_i \cdot \min_{\mu_1,\mu_2,\mu_3,\xi_p} (\xi_{mi}, \xi^*{}_{mi}) \tag{20}$$

where J represents the objective function to be maximized. It reflects the overall effectiveness of the TMD system in enhancing the structural damping. ρ_i is a weighting factor for the i-th mode, reflecting the relative importance of that mode's contribution to the overall structural response. ξ_{mi} and $\xi^*{}_{mi}$ are the additional conjugate modal damping ratio contributed by the TMD to the i-th mode of the structure obtained by Eq. (18).

The values are obtained through complex modal analysis of the combined structure-TMD system. It represents the increase in damping for each mode due to the TMD's presence. This approach is motivated by the understanding that even if some modes are well-damped, the overall structural response can still be significant if one critical mode has low damping.

The importance factors are used to consider the probability and importance of the occurrence of different modes. In this study, all modal vibrations are considered

Table 6 Optimal parameters of TMDs under different working conditions

Case		$\xi_p = 0\%$		$\xi_p = 1\%$		$\xi_p = 2\%$	
		γ_i^{opt}	ξ_i^{opt}	γ_i^{opt}	ξ_i^{opt}	γ_i^{opt}	ξ_i^{opt}
1TMD – μ_i = 1%		0.9901	0.0995	0.9891	0.1094	0.9881	0.1193
1TMD – μ_i = 2%		0.9804	0.1400	0.9790	0.1498	0.9776	0.1596
1TMD – μ_i = 3%		0.9709	0.1707	0.9692	0.1804	0.9676	0.1900
3TMDs – μ_i = 1%	1st	0.9891	0.1000	0.9881	0.1099	0.9871	0.1198
	2nd	0.9882	0.1010	0.9871	0.1109	0.9861	0.1209
	3rd	0.9876	0.1016	0.9865	0.1116	0.9854	0.1216
3TMDs – μ_i = 2%	1st	0.9781	0.1413	0.9767	0.1512	0.9753	0.1610
	2nd	0.9758	0.1441	0.9743	0.1540	0.9728	0.1639
	3rd	0.9735	0.1456	0.9720	0.1555	0.9704	0.1654
3TMDs – μ_i = 3%	1st	0.9672	0.1730	0.9655	0.1827	0.9637	0.1924
	2nd	0.9629	0.1778	0.9611	0.1876	0.9592	0.1974
	3rd	0.9581	0.1801	0.9561	0.1899	0.9541	0.1997
Field Installed TMD	1st	0.9702	0.1490	0.9687	0.1587	0.9672	0.1684
	2nd	0.9472	0.1869	0.9453	0.1964	0.9434	0.2060
	3rd	0.9228	0.2319	0.9203	0.2412	0.9178	0.2505

equally likely to occur and equally important, so all importance factors are set to 1. Global optimization of multiple TMDs is challenging and time-consuming because it involves many parameters and can easily solve for local optima. In this study, the Red-tailed hawk algorithm (RTH) is used as a computational framework to identify the optimal parameters of TMDs. This algorithm is developed to simulate the hunting behavior of a Red-tailed hawk, with the advantages of strong evolutionary ability, fast search speed, and strong optimization ability. This optimization method is particularly well suited for the target task because RTH avoids attempting local minima based on the Levy function (Ferahtia *et al.* 2023).

In this study, a typical steel pipe lightning rod is used as a case study. The dynamic parameters of the lightning rod are obtained by the field test. The optimal frequency ratio γ_i^{opt} and optimal damping ratio ξ_i^{opt} of the single-mode TMD and multi-mode TMD are calculated respectively. It should be noted that here only the first three modes of vibration are considered for multi-mode TMDs. The mass ratio μ_i is set to 1%, 2% and 3%, respectively, and the structural damping ratio ξ_p is set to 0%, 1% and 2%, respectively. At the same time, the TMD installed in the field is globally optimized and the results are compared in Table 6.

It can be seen from the table that with the increase of mass ratio μ, mode order i and structure damping ratio ξ_p, the optimal frequency ratio decreases, but the optimal damping ratio increases. The optimal frequency ratio of multiple TMDs is lower than that of a single TMD, because the mass of multiple TMDs leads to a decrease in structural frequency, and the optimal damping ratio of multiple TMDs is higher than that of a single TMD. For each order TMD mass given in this paper, it is necessary to set the corresponding optimal frequency ratio and optimal damping ratio by global optimization to ensure the optimal damping effect of TMD.

6. Conclusions

In response to the susceptibility of standalone lightning rods in substations to damage or even collapse under typical wind conditions, this study proposes an innovative approach by introducing a novel eddy current-tuned mass damper designed explicitly for vertical lightning rod structures. The TMD can effectively control wind-induced vibrations in the first three modes of the structure. Rigorous validation through on-site measurements confirms the exceptional vibration reduction performance of the proposed TMD. Several significant findings emerged from the analysis as follows:

- The modal frequencies of lightning rod obtained through the free vibration and environmental excitation methods in field measurement remain consistent. The identification error is generally within 5%. The independent lightning rod exhibits abundant identified frequencies and modal damping ratios below 3‰. The presence of low damping characteristics and closely spaced natural frequencies can easily excite micro wind-induced vibrations with multiple modes in the structure.
- The introduce of cantilever beams and pendulums as stiffness elements of the novel multi-mode TMD eliminates the need for springs and improves space efficiency. The introduce of eddy current damping technology mitigated potential maintenance challenges. Field test results verifies that the TMD can significantly reduce the RMS acceleration response of the original independent lightning rod by 50% and increase the modal damping ratio by 5‰ on average. The additional modal damping of the

fourth mode reaches 1%.

- There are significant differences in TMD design of large structures such as bridges or buildings, and flexible vertical structures such as steel pipe lightning rods. The additional mass of TMD device will cause the frequency of lightning rod to decrease greatly, which will affect the damping effect of TMD. The TMD design process considering the additional mass of the device is proposed to provide reference for similar projects.
- The state space equation of the TMD-structure model is established, and the TMD design steps considering the additional mass of the device are proposed based on the complex mode analysis. With the increase of mass ratio, mode order and structure damping ratio, the optimal frequency ratio decreases, but the optimal damping ratio increases. It is necessary to set the corresponding optimal frequency ratio and optimal damping ratio by global optimization to ensure the optimal damping effect of TMD.

Acknowledgments

The authors would like to greatly acknowledge the experimental facilities provided by the State Key Laboratory of Bridge Engineering Safety and Resilience in Hunan University, Hunan, China. This project has been financially supported by the National Natural Science Foundation of China (Grants NO. 52178477). The authors would like to thank the sponsors. Any opinion and conclusion presented in this paper are entirely those of the authors.

References

Caracoglia, L. and Jones, N.P. (2007), "Numerical and experimental study of vibration mitigation for highway light poles", *Eng. Struct.*, **29**(5), 821-831. https://doi.org/10.1016/j.engstruct.2006.06.023

Chen, W.-L., Min, X.-W. and Guo, Y.-J. (2022), "Performance of seal vibrissa-inspired bionic surface in suppressing aerodynamic forces and vortex shedding around a circular cylinder", *Ocean Eng.*, **260**, 112032. https://doi.org/10.1016/j.oceaneng.2022.112032

Christenson, R., Cashany, M., Hua, J. and Zuo, D. (2014), "Field testing of signal head vibration absorber to reduce fatigue in wind-excited traffic signal support structures", *Transport. Res. Record*, **2406**(1), 42-48. https://doi.org/10.3141/2406-05

Cook, R., Bloomquist, D., Richard, D. and Kalajian, M.A. (2001), "Damping of cantilevered traffic signal structures", *J. Struct. Eng.*, **127**, 1476-1483. https://doi.org/10.1061/(ASCE)0733-9445(2001)127:12(1476)

Constantinou, M.C., Soong, T.T. and Dargush, G.F. (1998), "Passive energy dissipation systems for structural design and retrofit".

Dao, T., Matsumiya, H., Noguchi, K., Xu, R., Marey, O. and Yagi, T. (2023), "Drag reduction of a cylinder by using spiral protuberances to generate three-dimensional surface flow", *J. Wind Eng. Industr. Aerodyn.*, **241**, 105550. https://doi.org/10.1016/j.jweia.2023.105550

Ferahtia, S., Houari, A., Rezk, H., Djerioui, A., Machmoum, M., Motahhir, S. and Ait-Ahmed, M. (2023), "Red-tailed hawk algorithm for numerical optimization and real-world problems". *Scientif. Reports*, **13**(1), 12950. https://doi.org/10.1038/s41598-023-38778-3

Hamilton III, H.R., Riggs, G.S. and Puckett, J.A. (2000), "Increased damping in cantilevered traffic signal structures", *J. Struct. Eng.*, **126**(4), 530-537. https://doi.org/10.1061/(ASCE)0733-9445(2000)126:4(530)

Han, Y., Zhou, X., Wang, L., Cai, C.S., Yan, H. and Hu, P. (2021), "Experimental investigation of the vortex-induced vibration of tapered light poles", *J. Wind Eng. Industr. Aerodyn.*, **211**, 104555. https://doi.org/10.1016/j.jweia.2021.104555

Kontoni, D.-P.N. and Farghaly, A.A. (2020), "TMD effectiveness for steel high-rise building subjected to wind or earthquake including soil-structure interaction", *Wind Struct., Int. J.*, 30(4), 423-432. https://doi.org/10.12989/was.2020.30.4.423

Liu, M., Li, S. and Chen, Z. (2020), "Mitigation of wind-induced responses of cylinder solar tower by a tiny eddy current tuned mass damper based on elastic wind tunnel tests", *Smart Struct. Syst., Int. J.*, **26**(5), 619-629. https://doi.org/10.12989/sss.2020.26.5.619

Maryami, R., Arcondoulis, E.J.G., Guo, J. and Liu, Y. (2024), "Experimental investigation of active local blowing on the aerodynamic noise reduction of a circular cylinder", *J. Sound Vib.*, **578**, 118360. https://doi.org/10.1016/j.jsv.2024.118360

Mengistu, M.T., Orlando, A. and Repetto, M.P. (2023), "Wind and structural response monitoring of a lighting pole for the study of downburst effects on structures", *J. Wind Eng. Industr. Aerodyn.*, **240**, 105447. https://doi.org/10.1016/j.jweia.2023.105447

Mcmanus, P., Hamilton, H. and Puckett, J. (2003), "Damping in Cantilevered Traffic Signal Structures under Forced Vibration", *J. Struct. Eng.*, **129**, 373-382. https://doi.org/10.1061/(ASCE)0733-9445(2003)129:3(373)

Nguyen, C.H., Freda, A., Solari, G. and Tubino, F. (2015), "Aeroelastic instability and wind-excited response of complex lighting poles and antenna masts", *Eng. Struct.*, **85**, 264-276. https://doi.org/10.1016/j.engstruct.2014.12.015

Pagnini, L.C. and Solari, G. (2001), "Damping measurements of steel poles and tubular towers", *Eng. Struct.*, **23**(9), 1085-1095. https://doi.org/10.1016/S0141-0296(01)00011-6

Quen, L.K., Abu, A., Kato, N., Muhamad, P., Tan, L.K. and Kang, H.S. (2018), "Performance of two- and three-start helical strakes in suppressing the vortex-induced vibration of a low mass ratio flexible cylinder", *Ocean Eng.*, **166**, 253-261. https://doi.org/10.1016/j.oceaneng.2018.08.008

Repetto, M.P. and Solari, G. (2010), "Wind-induced fatigue collapse of real slender structures", *Eng. Struct.*, **32**(12), 3888-3898. https://doi.org/10.1016/j.engstruct.2010.09.002

Solari, G. and Pagnini, L.C. (1999), "Gust buffeting and aeroelastic behaviour of poles and monotubular towers", *J. Fluids Struct.*, **13**(7-8), 877-905. https://doi.org/10.1006/jfls.1999.0240

Tapia-Hernández, E. (2016), "Tubular steel poles under lateral load patterns", *Adv. Steel Constr.*, **12**(4), 428-445. https://doi.org/10.18057/IJASC.2016.12.4.4

Thiyagarajan, J.S., Siringoringo, D.M., Wangchuk, S. and Fujino, Y. (2021), "Implementation of video motion magnification technique for non-contact operational modal analysis of light poles", *Smart Struct. Syst., Int. J.*, **27**(2), 227-239. https://doi.org/10.12989/sss.2021.27.2.227

Wen, Q., Hua, X.G., Chen, Z.Q., Niu, H.W. and Wang, X.Y. (2018), "AMD-based random decrement technique for modal identification of structures with close modes", *J. Aerosp. Eng.*, **31**(5), 04018057. https://doi.org/10.1061/(ASCE)AS.1943-5525.0000882

Xu, C., Gu, X., Mao, Y. and Wang, C. (2024), "Experimental

studies on simultaneously reducing flow drag and noise of a circular cylinder with a downstream porous material plate", *Experim*. *Thermal Fluid Sci*., **155**, 111209. https://doi.org/10.1016/j.expthermflusci.2024.111209

Zhao, G., Li, J., Zhang, M. and Yi, Y. (2022), "Experimental study on the bearing capacity and fatigue life of lightning rod structure joints in high-voltage substation structures", *Thin-Wall*. *Struct*., **175**, 109282. https://doi.org/10.1016/j.tws.2022.109282

Zhou, Z., Xie, Z. and Zhang, L. (2023), "Vibration control in high-rise buildings with tuned liquid dampers - Numerical simulation and engineering applications", *Wind Struct*., *Int*. *J*., **36**(2), 91-103. https://doi.org/10.12989/was.2023.36.2.091